



Original Article

The Evident of Coupled Spin and Electron-phonon Interactions in $\text{Cd}_2\text{Os}_2\text{O}_7$ Pyrochlore

Le Duc Huy¹, Nguyen Xuan Nghia¹, Nguyen Thi Huyen¹,
Vu Thi Kim Oanh², Nguyen Van Minh³, Nguyen Thi Minh Hien^{1,*}

¹*Institute of Physics, Vietnam Academy of Science and Technology, 18 Hoang Quoc Viet, Hanoi, Vietnam*

²*Graduate University of Science and Technology, Vietnam Academy of Science and Technology,
18 Hoang Quoc Viet, Hanoi, Vietnam*

³*Hanoi National University of Education, 136 Xuan Thuy, Cau Giay, Hanoi, Vietnam*

Received 30 December 2022

Revised 28 March 2023; Accepted 6 April 2023

Abstract: We present the results of the temperature dependence of the Raman spectra of pyrochlore $\text{Cd}_2\text{Os}_2\text{O}_7$ single crystal in a temperature range of 100 -270 K. We found that, among the six observed Raman active modes, the 762 cm^{-1} phonon has a significant peak shift and asymmetric Fano lineshape. The temperature-dependent of the frequency and full width at half maximum (FWHM) of the phonon shows the kinks near the Néel temperature. The complex temperature-dependent asymmetry Fano parameter and the anomalies of the FWHM below Néel temperature indicate coupling of the 762 cm^{-1} phonon to both electron and spin degrees of freedom. In addition, we found the Fano asymmetry rapidly drops below the Néel temperature towards its minimum value of $\sim 200\text{ K}$. Thus, at temperature ranging from 200 K to T_N , the pyrochlore is suggested to be in an all-in -all-out ordered semimetallic state. We also confirm that Raman scattering temperature dependence provides a simple and powerful method for investigating temperature transitions and coupling in pyrochlore materials.

Keywords: Metal-insulator transition, electron-phonon coupling, spin-phonon coupling, Raman scattering.

1. Introduction

The pyrochlore $\text{Cd}_2\text{Os}_2\text{O}_7$ belongs to the class of metal–insulator transition (MIT) materials characterized by a high-temperature metallic state that is transformed into a low-temperature insulating

* Corresponding author.

E-mail address: ntmhien@iop.vast.vn

<https://doi.org/10.25073/2588-1124/vnumap.4798>

state at a critical temperature [1-5]. It carries important information about the fundamental property of electrons in crystals, since it is caused by certain electronic instabilities associated with Coulomb interactions among electrons, Fermi-surface instability, or couplings to other degrees of freedom. The MIT is significant for technological applications such as sensors and switching devices, in addition to the academic interest, because rapid changes in resistivity and optical absorption at the transition are advantageous for them.

The coupling between various degrees of freedom (spin, electron, lattice, and orbital) is a key paradigm in condensed matter physics. It is known that such couplings can result in novel ground states and various emergent phenomena [6-9]. Recently, there has been a rise in interest in spin-phonon coupling and electron-phonon coupling in the context of multiferroics and spintronics, which also provide the opportunity to introduce novel functionality in transition metal oxides.

In the $5d$ transition metal oxide pyrochlores, a continuous metal-insulator transition is often accompanied by all-in-all-out antiferromagnetic order. The Os spins in a given Os-O tetrahedron point inward (all-in), while those in the neighboring tetrahedra point outward (all-out). The extended nature of the $5d$ Os orbitals in a regime of intermediate electron correlation and large spin-orbit interaction means that this system may host several novel or topological states of matter. Due to the fact that AIAO order breaks time-reversal symmetry while maintaining the crystalline symmetry of the pyrochlore lattice, the intimate link between AIAO order and electronic structure is particularly noteworthy. The AIAO magnetic ordering at the Os sites has been firmly established by resonant X-ray and neutron diffraction below $T_N = 227$ K.

Raman scattering is a unique technique for characterization and quantification of electron-phonon, spin-phonon and spin-lattice coupling in many of the many compounds like multiferroics and manganites. Our results show that the temperature dependence of Raman scattering can be simple and powerful quantity for investigating the temperature transitions as well as the coupling between spin, charge and lattice vibration. In this work, we present a study of phonon hardening of 762 cm^{-1} phonon which is the strongest Raman-active mode in pyrochlore $\text{Cd}_2\text{Os}_2\text{O}_7$ single crystal through temperature dependent Raman scattering. We discuss that the major contribution of the phonon hardening and the anomalous behavior of asymmetry Fano parameter would involve to spin-phonon coupling and electron-phonon coupling.

2. Experimental

2.1. Sample Preparation

Pyrochlore $\text{Cd}_2\text{Os}_2\text{O}_7$ single crystal was grown by the chemical transport method. In the beginning, a polycrystalline pellet was prepared from a mixture including CdO and Os in a sealed quartz tube with a suit amount of AgO serving as the oxygen source at 1073 K. Second, a temperature gradient of 1040-1200 K was maintained in the furnace for a week with the pellet on the side with the higher temperature. Single crystals were then grown via a chemical vapor transport process.

2.2. Raman Scattering

Raman scattering spectra of the samples were obtained in a backscattering configuration with microprobe LabRam HR Evolution Raman spectrometers. The 632 nm laser line was used as the excitation source with a laser power of ~ 1 mW on the surface of the sample. The beam power density was low enough to avoid laser heating in the measured temperature range. A 632 nm edge filter was used so that the spectrum at wavenumbers below 100 cm^{-1} was blocked. The sample was mounted in a

compact temperature stage (Linkam THMS600) for the temperature-dependent measurement from 80 K to 300 K.

3. Results and Discussion

3.1. The First Order Phonon of $\text{Cd}_2\text{Os}_2\text{O}_7$

$\text{Cd}_2\text{Os}_2\text{O}_7$ pyrochlore structure belongs to cubic space group $Fd\bar{3}m$ and $m\bar{3}m$ point-group with eight formula units per primitive cell. By making the correlation between site group and factor group for each site, and then eliminating the acoustic mode, we obtain the vibrational modes of $\text{Cd}_2\text{Os}_2\text{O}_7$: $\Gamma = A_{1g} + E_g + 7T_{1u} + 4T_{2g} + 4T_{2u} + 3E_u + 2T_{1g} + 2A_{2u}$. The infrared (IR)-active vibrational modes have the $7T_{1u}$ symmetry, whereas the Raman-active modes have the A_{1g} , $4T_{2g}$, and E_g symmetries.

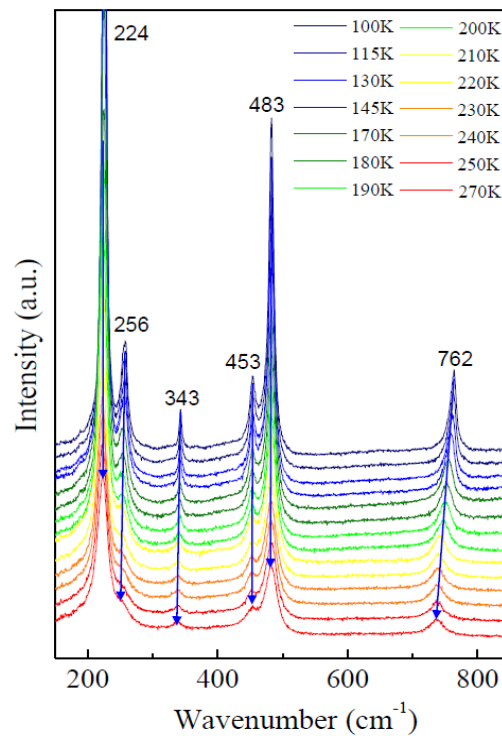


Figure 1. The temperature-dependent Raman spectra of $\text{Cd}_2\text{Os}_2\text{O}_7$ obtained from 100 K to 270 K under 633 nm laser excitation.

Figure 1 shows the temperature-dependent Raman spectra of pyrochlore $\text{Cd}_2\text{Os}_2\text{O}_7$ single crystal obtained from 100 K to 270 K. We observed six phonon modes at ~ 224 ; 256; 343; 453; 483 and 762 cm^{-1} . The six observed Raman peaks well agree with the reported experimental and theoretical values of the phonon modes of $\text{Cd}_2\text{Os}_2\text{O}_7$ pyrochlore [10, 11]. By comparison with the previous reports, the four peaks at 224; 343; 453 and 762 cm^{-1} can be assigned to T_{2g} , the peak at 256 cm^{-1} to E_g and the peak at 483 cm^{-1} to A_{1g} . The sample shows similar Raman scattering peaks from 100 K to 270 K, which implies that the space group in the low-temperature phase is the same as that in the high-temperature phase, $Fd\bar{3}m$. Our Raman results also well agree with the previous XRD studies of the crystal structure

of the $\text{Cd}_2\text{Os}_2\text{O}_7$ samples [12]. As a result, we draw the conclusion that in this compound, spatial symmetry breaking does not take place along the transition from low to room temperature.

From Figure 1, all six phonon modes shift to a lower frequency when the temperature increases. The most interesting feature is that when the temperature changes from 100 K to 270 K, while other phonons shift only a few cm^{-1} , the 762 cm^{-1} phonon (Ph6) shows significant shifting, about $\sim 30 \text{ cm}^{-1}$. In addition, this phonon mode has asymmetry lineshape. This clearly indicates the presence of strong interactions between the electronic background and the phonon modes.

3.2. The Vibration of 762 cm^{-1} Phonon Mode

Now we focus on the strongest shift Raman-active 762 cm^{-1} phonon mode. The crystal structure of $\text{A}_2\text{B}_2\text{O}_7$ compounds depends on ionic radius ratio of r_A and r_B [13]. The most commonly seen structures are cubic pyrochlore and defective fluorite phases, and sometimes a monoclinic phase exists. When $r_A/r_B = 1.46 - 1.78$, pyrochlore structure steadily exists [14]. $\text{Cd}_2\text{Os}_2\text{O}_7$ crystallizes in the cubic $\text{Fd}\bar{3}\text{m}$ space group. Os^{5+} forms OsO_6 octahedra by bonding with six equivalent O^{2-} ions, and these octahedra share edges with six equivalent CdO_8 hexagonal bipyramids. Cd^{2+} is bonded to eight O^{2-} atoms to form distorted CdO_8 hexagonal bipyramids that share edges with six equivalent CdO_8 hexagonal bipyramids and edges with six equivalent OsO_6 octahedra. Cd-O bonds come in two shorter and six longer bond lengths, lead to two different sites for Oxygen. In the first site, O(1) is bonded to four equivalent Cd^{2+} atoms to form corner-sharing OCd_4 tetrahedra, while in the second site, O(2) is bonded in a 4-coordinate geometry to two equivalent Os^{5+} and two equivalent Cd^{2+} atoms [15].

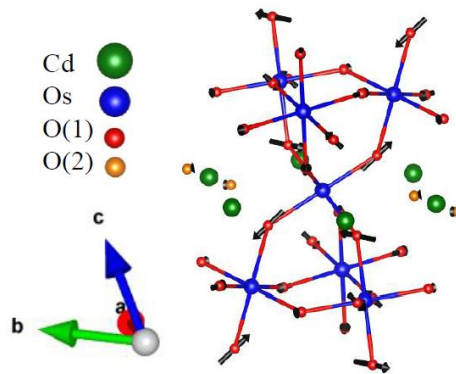


Figure 2. Schematic representation of the eigenvector for 762 cm^{-1} phonon mode. Cd, Os, O(1) and O(2) atoms are represented by the green, blue, red and yellow balls. The arrows show the directions and the amplitudes of the atomic displacements of the mode.

The first-principles calculations were performed using density functional theory +U with the PBEsol exchange correlation functional. Based on the phonon eigen modes from first-principles calculation, Figure 2 represents of the eigenvectors for the most Raman active phonon mode. As can be seen in Fig. 2, 762 cm^{-1} phonon mode corresponds to stretching modes, in which the O(1) atom displacements are mainly along the direction of the Os-Os bond. It also agrees well with the report of B. H. Zhang et al., [16]. The basic electronic properties of the metallic state are determined by three $5d$ electrons in the t_{2g} manifold of the Os^{5+} ions, which form a semimetallic band [3]. Since Sleight and colleagues reported a sharp increase in resistivity below 225 K, the osmium pyrochlore oxide $\text{Cd}_2\text{Os}_2\text{O}_7$ has been known to undergo a metal-insulator transition [17]. Mandrus and coworkers reviewed the MIT

of $\text{Cd}_2\text{Os}_2\text{O}_7$ and show that it is a continuous, second-order transition accompanied by noncollinear all-in/all-out (AIAO) magnetic order. The magnetic transition as well as the metal-insulator transitions would affect the Os-O bond in OsO_6 octahedra. At this temperature, the phonon mode correlated to vibration of O-Os bonds in OsO_6 may exhibit anomalous phonon frequency changes at this temperature.

3.3. Spin-phonon Coupling and Electron-phonon Coupling of 762 cm^{-1} Phonon Mode

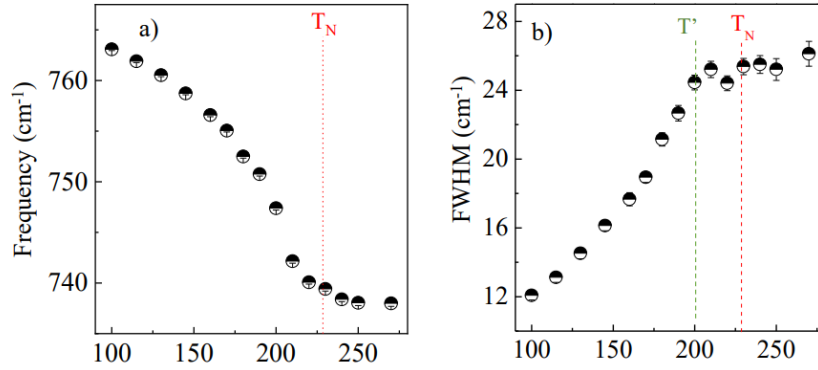


Figure 3. The temperature-dependent of the frequency shift (a) and the full width at half maximum (b). The experimental data are plotted in symbols and fitted model are shown in dot lines.

To understand the anomalous behavior of Ph6, we study the temperature dependence of phonon frequency and FWHM. As can be seen in Figure 3, the Ph6 mode has anomalous temperature-dependent behavior. The anomalous temperature dependence of the phonon frequency would indicate a phase transition near $\sim 227\text{ K}$ in pyrochlore $\text{Cd}_2\text{Os}_2\text{O}_7$. Both experimental observations and theoretical calculations suggest magnetic and metal-insulator transitions of $\text{Cd}_2\text{Os}_2\text{O}_7$ near the same temperature.

In magnetic materials, the frequency change of a phonon mode with temperature can be written as [18].

$$\omega = \omega_0 + \Delta\omega_{\text{latt}} + \Delta\omega_{\text{anh}} + \Delta\omega_{\text{e-ph}} + \Delta\omega_{\text{s-ph}} \quad (1)$$

The first term on the right-hand side is the harmonic frequency of the phonon. The second term is the contribution of the lattice expansion/contraction to the phonon frequency. The intrinsic anharmonic contribution is the third term. The fourth term accounts for the effect of renormalization of the phonon frequency due to electron-phonon coupling. And the contribution of spin-phonon coupling, which results from the modulation of the exchange integral by lattice vibrations, is represented by the last component. In general, especially at low temperatures, the lattice expansion contribution is significantly less than the intrinsic anharmonic contribution. Normally, a phonon can decay into two or three phonons, with a higher probability of the former. In the phonon decay, conservation of energy and momentum has to be obeyed, with a higher probability of decaying into same energy phonons. The anharmonic contribution for two-channel phonon decay with the same energies can be expressed as:

$$\Delta\omega_{\text{anh}} = -A \left(1 + \frac{2}{e^{\frac{\hbar\omega_0}{2k_B T}} - 1} \right) \quad (2)$$

where A is an anharmonic constant. The $\omega_0 + \Delta\omega_{\text{anh}}$ is a smooth function of temperature and can not explain the anomalies at T_N . Note that the $\Delta\omega_{\text{e-ph}}$ is generally negative [19, 20], while the $\Delta\omega_{\text{s-ph}}$ can be positive or negative depending on the detailed magnetic Hamiltonian and phonon modes. In $\text{Cd}_2\text{Os}_2\text{O}_7$,

the hardening of Ph6 indicates that both the electron-phonon coupling and the spin-phonon coupling could, in principle, be the origin of the observed anomalies at T_N .

The Ph6 shows a distinct asymmetric lineshape. This type of spectral lineshape can arise from the coupling of the phonon with a continuum of excitations and is frequently seen in the Raman spectra of metal. Figure 1 illustrates how the Ph6 exhibits a Fano asymmetry at temperatures higher than T_N . We have fitted the T-dependent spectra with the Breit-Wigner-Fano profile to quantify the observed alteration [21]:

$$I(\omega) = I_0 \frac{[1 + (\omega - \omega_0)/q\Gamma]^2}{1 + [(\omega - \omega_0)/\Gamma]^2} \quad (3)$$

Here I_0 is the intensity, ω_0 is the phonon frequency, Γ is the FWHM and $1/|q|$ is Fano asymmetry parameter of the Breit-Wigner-Fano mode. As the peak becomes more asymmetric, “q” decreases. The inverse of the asymmetry parameter ($1/|q|$) is a measure of metallicity in the system [22]. The Fano fitting adequately describes the Ph6 phonon from 100 to 270 K, as shown in Figure 4. It is observed that the Fano parameter decrease as the temperature decreases. The interesting thing is that the temperature-dependent of Fano asymmetry parameter shows a clear kink at ~ 200 K. In the metallic region about $T_N \sim 227$ K, $1/|q|$ remains constant and quite large, indicating that the Ph6 is strongly coupled with free carriers. At $T < 200$ K, $|q|$ is approximately proportional to temperature, implying the coupling to spin degrees of freedom as well. At temperature between 200 and 227 K, the value of $|q|$ may be understood by combining these two couple contributions. Therefore, the transition can be explained like that:

i) Above the transition point (T_N): due to the even number of electrons in the unit cell, the system is in a paramagnetic semimetallic state with an equal number of electrons and holes. In particular, the energy of the electron and hole bands are overlaps, creating a semimetallic state. Both electrons and hole bands at the Fermi level (E_F), leading to a large $1/|q|$ due to electron-phonon coupling;

ii) From T_N to $T' \sim 200$ K: When the temperature decreases and passes through T_N , the appearance of all-in-all-out ordering causes the electron and hole bands to shift upward and downward, respectively, progressively annihilating the Fermi surface. In other words, as the magnetic order develops, the electron and hole bands are repelled from E_F and the electronic contribution to $1/|q|$ becomes gradually reduced. The electron and hole pockets disappear, and their overlap in energy eventually becomes zero at $T' \sim 200$ K;

iii) Below $T' \sim 200$ K: A solid insulating phase results from the development of a genuine energy gap between the electron and hole bands. The Fermi surface is entirely removed, and $1/|q|$ rapidly drops to its minimum value.

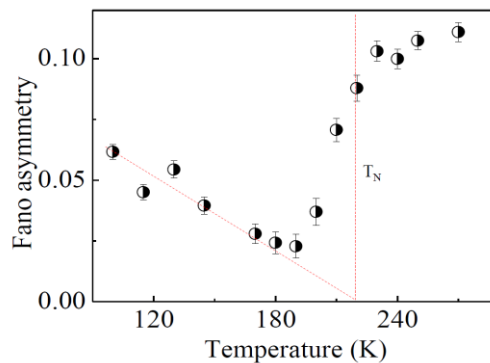


Figure 4. The temperature- dependence of Fano asymmetry parameter. The experimental data are plotted in symbols. The dashed lines are guides for the eye.

4. Conclusion

We have presented the results of the Raman studies for the pyrochlore $\text{Cd}_2\text{Os}_2\text{O}_7$ single crystal. We found the hardening and asymmetry phonon at 762 cm^{-1} , relating with the stretching modes, in which the O(1) atom displacements are primarily along the Os-Os bond direction. The temperature dependence of both phonon frequency and FWHM shows anomalous temperature changes below T_N . The possible origins of phonon hardening are discussed, and we propose that spin-phonon coupling and electron-phonon coupling contribute significantly to the couples to 762 cm^{-1} phonon. In addition, we found the Fano asymmetry rapidly drops below the Néel temperature towards its minimum value of $\sim 200\text{ K}$. This suggests that when the temperatures increase from 100 K to 270 K , the pyrochlore exists in three states: AIAO insulator (below 200 K), AIAO ordered semimetallic ($200\text{ K} - T_N$) and P-semimetallic states (above T_N). We also confirm that the temperature dependence study of Raman scattering provides a simple and powerful method for investigating the temperature transitions, as well as the coupling in pyrochlore materials.

Declaration of Competing Interest

The authors declare that they have no known competing financial interests or personal relationships that could have appeared to influence the work reported in this paper.

Acknowledgment

This research is funded by Vietnam National Foundation for Science and Technology Development (NAFOSTED) under grand number 103.02-2018.39. We are grateful for the use of facilities of the joint optics lab (between IOP and GUST, VAST) and photonics lab at IOP, VAST.

References

- [1] V. G. Sathe, S. Tyagi, G. Sharma, Electron-phonon Coupling in Perovskites Studied by Raman Scattering, *J. Phys. Conf. Ser.*, Vol. 755, 2016, pp. 012008, <https://doi.org/10.1088/1742-6596/755/1/012008>.
- [2] N. A. Bogdanov, R. Maurice, I. Rousochatzakis, J. V. D. Brink, L. Hozoi, Magnetic State of Pyrochlore $\text{Cd}_2\text{Os}_2\text{O}_7$ Emerging from Strong Competition of Ligand Distortions and Longer-Range Crystalline Anisotropy, *Phys. Rev. Lett.*, Vol. 110, 2013, pp. 127206, <https://doi.org/10.1103/PhysRevLett.110.127206>.
- [3] Z. Hiroi, J. Yamaura, T. Hirose, I. Nagashima, Y. Okamoto, Lifshitz Metal-insulator Transition Induced by the All-in/all-out Magnetic Order in the Pyrochlore Oxide $\text{Cd}_2\text{Os}_2\text{O}_7$, *APL Materials*, Vol. 3, 2015, pp. 041501, <https://doi.org/10.1063/1.4907734>.
- [4] J. W. Lynn, L. V. Doloc, Spin Dynamics of the Magnetoresistive Pyrochlore $\text{Tl}_2\text{Mn}_2\text{O}_7$, *Phys. Rev. Lett.*, Vol. 80, 1998, pp. 4582-4585, <https://doi.org/10.1103/PhysRevLett.80.4582>.
- [5] W. J. Padilla, D. Mandrus, D. N. Basov, Searching for the Slater Transition in the Pyrochlore $\text{Cd}_2\text{Os}_2\text{O}_7$ with Infrared Spectroscopy, *Phys. Rev. B*, Vol. 66, 2002, pp. 035120, <https://doi.org/10.1103/PhysRevB.66.035120>.
- [6] D. I. Khomskii, G. A. Sawatzky, Interplay Between Spin, Charge and Orbital Degrees of Freedom in Magnetic Oxides, *Solid State Commun.* Vol. 102, 1997, pp 87-99, [https://doi.org/10.1016/S0038-1098\(96\)00717-X](https://doi.org/10.1016/S0038-1098(96)00717-X).
- [7] A. Lanzara, P.V. Bogdanov, X. J. Zhou, S. A. Kellar, D. L. Feng, E. D. Lu, T. Yoshida, H. Eisaki, A. Fujimori, K. Kishio, J. I. Shimoyama, T. Noda, S. Uchida, Z. Hussain, Z. X. Shen. Evidence for Ubiquitous Strong Electron-phonon Coupling in High-temperature Superconductors, *Nature*, Vol. 412, 2021, pp. 510-514, <https://doi.org/10.1038/35087518>.
- [8] Y. Tokura, N. Nagaosa, Orbital Physics in Transition-metal Oxides, *Science*, Vol. 288, 2000, pp. 462-468, <https://doi.org/10.1126/science.288.5465.462>.

- [9] M. Mochizuki, N. Furukawa, N. Nagaosa, Theory of Spin-phonon Coupling in Multiferroic Manganese Perovskites RMnO_3 . *Phys. Rev. B*, Vol. 84, 2011, pp. 144409, <https://doi.org/10.1103/PhysRevB.84.144409>.
- [10] M. Glerup, O. F. Nielsen, F. W. Poulsen, The Structural Transformation from the Pyrochlore Structure, $\text{A}_2\text{B}_2\text{O}_7$, to the Fluorite Structure, AO_2 , Studied by Raman Spectroscopy and Defect Chemistry Modeling, *J. Solid State Chem.*, Vol. 160, 2001, pp 25-32, <https://doi.org/10.1006/jssc.2000.9142>.
- [11] Y. Wang, T. F. Rosenbaum, A. Palmer, Y. Ren, J. W. Kim, D. Mandrus, Y. Feng, Strongly-coupled Quantum Critical Point in an All-in-all-out Antiferromagnet, *Nat Commun*, Vol. 9, 2018, pp. 2953, <https://doi.org/10.1038/s41467-018-05435-7>.
- [12] J. Yamaura, K. Ohgushi, H. Ohsumi, T. Hasegawa, I. Yamauchi, K. Sugimoto, S. Takeshita, A. Tokuda, M. Takata, M. Udagawa, M. Takigawa, H. Harima, T. Arima, Z. Hiroi, Tetrahedral Magnetic Order and the Metal-Insulator Transition in the Pyrochlore Lattice of $\text{Cd}_2\text{Os}_2\text{O}_7$, *Phys. Rev. Lett.*, Vol. 108, 2012, pp. 247205, <https://doi.org/10.1103/PhysRevLett.108.247205>
- [13] Z. Wang, G. Zhou, D. Jiang, S. Wang, Recent Development of $\text{A}_2\text{B}_2\text{O}_7$ System Transparent Ceramics, *Journal of Advanced Ceramics*, Vol. 7, 2018, pp.289-306, <http://dx.doi.org/10.1007/s40145-018-0287-z>.
- [14] M. A. Subramanian, G. Aravamudan, G. V. S. Rao, Oxide Pyrochlores - A Review, *Progress in Solid State Chemistry*, Vol. 15, 1983, pp. 55-143, [https://doi.org/10.1016/0079-6786\(83\)90001-8](https://doi.org/10.1016/0079-6786(83)90001-8).
- [15] J. Xu, R. Xi, X. Xu, Y. Zhang, X. Feng, X. Fang, X. Wang, $\text{A}_2\text{B}_2\text{O}_7$ Pyrochlore Compounds: A Category of Potential Materials for Clean Energy and Environment Protection Catalysis, *Journal of Rare Earths*, Vol. 38, 2020, pp. 840-849, <https://doi.org/10.1016/j.jre.2020.01.002>.
- [16] B. H. Zhang, Z. Wang, R. Q. Wu, First-principles Studies of the Unconventional Spin-phonon Coupling Mediated by Spin-orbit Coupling in Pyrochlore $\text{Cd}_2\text{Os}_2\text{O}_7$, *Phys. Rev. B*, Vol. 104, 2021, pp. 024411, <https://doi.org/10.1103/PhysRevB.104.024411>.
- [17] A. W. Sleight, J. L. Gilson, J. F. Weiher, W. Bindloss, Semiconductor-metal Transition in Novel $\text{Cd}_2\text{Os}_2\text{O}_7$, *Solid State Commun*, Vol. 14, 1974, pp. 357-359, [https://doi.org/10.1016/0038-1098\(74\)90917-X](https://doi.org/10.1016/0038-1098(74)90917-X).
- [18] E. Granado, A. Garcia, J. A. Sanjurjo, C. Rettori, I. Torriani, F. Prado, R. D. Sanchez, A. Caneiro, S. B. Oseroff, Magnetic Ordering Effects in the Raman spectra of $\text{La}_{1-x}\text{Mn}_{1-x}\text{O}_3$, *Phys. Rev. B*, Vol. 60, 1999, pp. 11879, <https://doi.org/10.1103/PhysRevB.60.11879>.
- [19] M. Reizer, Screening Effects in the Electron–optical-phonon Interaction, *Phys. Rev. B*, Vol. 61, 2000, pp. 40-42, <https://doi.org/10.1103/PhysRevB.61.40>.
- [20] D. Olego, M. Cardona, Self-energy Effects of the Optical Phonons of Heavily Doped p–GaAs and p–Ge, *Phys. Rev. B*, Vol. 23, 1981, pp. 6592-6602, <https://doi.org/10.1103/PhysRevB.23.6592>.
- [21] E. H. Hasdeo, A. R. T. Nugraha, K. Sato, M. S. Dresselhaus, R. Saito, Electronic Raman Scattering and the Fano Resonance in Metallic Carbon Nanotubes, *Phys. Rev. B*, Vol. 88, 2013, pp. 115107, <https://doi.org/10.1103/PhysRevB.88.115107>.
- [22] C. Hartinger, F. Mayr, A. Loidl, T. Kopp, Cooperative Dynamics in Doped Manganite Films: Phonon Anomalies in the Ferromagnetic State, *Phys. Rev. B*, Vol. 70, 2004, pp. 134415, <https://doi.org/10.1103/PhysRevB.70.134415>.